An Improved Mimetic Compound for Styrene "Living" Free Radical Polymerization. An Initiator Containing the "Penultimate" Unit

W. G. Skene, J. C. Scaiano,* and Glenn P. A. Yap

Department of Chemistry, University of Ottawa, Ottawa K1N 6N5, Canada

Received November 15, 1999; Revised Manuscript Received February 16, 2000

ABSTRACT: A new thermal initiator for living free radical polymerization (LFRP) has been synthesized photochemically by coupling of the free radical TEMPO with the 1,3-diphenyl-1-propyl radical. This initiator (**4**), which contains the penultimate monomer unit, is a much better mimetic compound than similar compounds derived from radicals with a single styrene moiety, such as the 1-phenylethyl radical (which yields adduct **2**). In particular, **4** does not yield any disproportionation products, while other model compounds usually do. This is attributed to the lowest energy conformation of **4**, which places the β-hydrogen atoms in an unfavorable stereoelectronic arrangement to give disproportionation products. It is anticipated that the same situation will prevail in the polymer, and it is instrumental in determining the low polydispersities achievable with LFRP. This report includes a detailed study of the properties of **4**, including its thermal decomposition and relevant free radical kinetics, as well as a comparison of the rotational barrier of **4** with that of **2**.

The methodology of "living" free radical polymerization (LFRP) has been the subject of considerable interest since it offers the possibility of controlling polydispersity in free radical polymerization, and of the convenient design of block copolymers.[1,2] Nitroxide radicals have long been known to be excellent carbon radical scavengers,[3] and the LFRP strategy, initially introduced by Rizzardo and co-workers[4,5] was originally used to advantage in the control of polydispersities by Georges et al.[6,7] The "living" properties of LFRP derive from the reversible capping of the growing polymer chain, as indicated in Scheme 1. The reversibility arises from the

Scheme 1

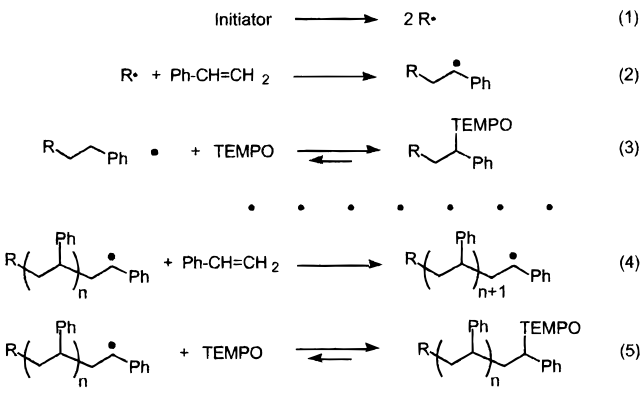

low values of the C−O bond dissociation energies (BDE), which for model compounds (vide infra) have been measured around 117 kJ/mol.[8−10] The control of the nitroxide concentration during polymerization has proven a key parameter in determining the properties of the resulting polymers.[6,11,12] A number of convenient stoichiometric initiators have been developed; among them, alkoxyamines **1**−**3** have proven convenient.

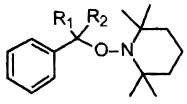

1: $R_1 = R_2 = H$
2: $R_1 = H; R_2 = CH_3$
3: $R_1 = R_2 = CH_3$

In addition to being convenient initiators for LFRP, these alkoxyamines also provide useful models for the capping−decapping of the polymer systems. In particular, **2** offers the best mimetic properties, given the styrene moiety it contains and the secondary benzylic radical it forms upon C−O cleavage. This mimetic property comes into question when one observes the thermal decomposition of these compounds; for example, **2** gives styrene and the hydroxylamine shown in reaction 6.

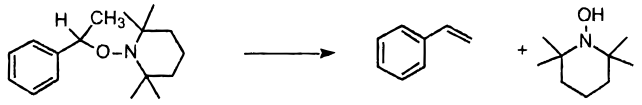

(6)

In the absence of radical scavengers, reaction 6 is the main pathway for the decomposition of **2**. In the presence of radical scavengers, such as monomers,[13] oxygen,[14] or other nitroxides,[8] decomposition of alkoxyamines occurs faster and gives other products, indicative of scavenging of carbon-centered radicals, along with small amounts of disproportionation products.[8,14,15] The difference in behavior, particularly the relative thermal stability of alkoxyamines in the absence of scavengers can be readily explained with the Fischer−Ingold persistent free radical effect, which in this case favors cross combination of the radicals to regenerate the starting material.[16−18] Studies in the presence of scavengers show that at 125 °C 3% of the cleavage-capping processes lead to disproportionation products for **2**, while for **3**, the fraction is ∼5%.[8] To the extent that **2** may be a good model for the polymer itself, 3% disproportionation products would imply that LFRP cannot be a suitable way of controlling polymer polydispersities.

Since LFRP is indeed an excellent way of controlling polydispersities, one must conclude that thermal decomposition of **2** does not mimic well the formation of disproportionation products. We note that the same arguments apply whether disproportionation products are formed by actual radical disproportionation (in- or out-of-cage), or through a concerted process. Since

10.1021/ma991924d CCC: $19.00
Published on Web 04/27/2000

Scheme 2

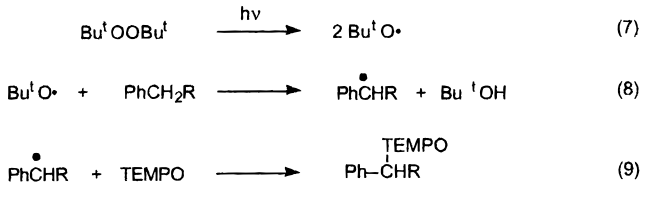

working directly with the polymer or oligomers is impractical (particularly if crystallographic information is desired), we synthesized compound **4**, to which we

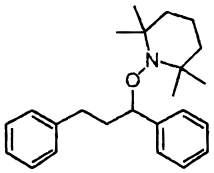

4

refer as the "penultimate" model initiator since it contains essentially two styrene moieties.[19] The results obtained demonstrate that **4** has excellent mimetic properties, and its study leads to a clear rationalization for the absence of disproportionation in the actual polymerization process.

As part of this work, we have also determined the characteristics of **4** from the point of view of its thermal decomposition, as well as the relevant free radical kinetics.

Results

Synthesis. Initiators such as **1**−**3** can be readily prepared by photolysis of di-*tert*-butyl peroxide in the precursor hydrocarbon in the presence of the nitroxide.[20] Bleaching of the nitroxide color serves as an indicator of reaction completion, Scheme 2.

The photochemical synthesis of **4** was not as straightforward as those for the benzylic analogues (e.g. **1**−**3**) prepared previously. Typically, the precursor hydrocarbon is used as solvent; however, in the case of 1,3-diphenylpropane this is impractical because of its low volatility, high viscosity, and high cost. Typical yields, with stoichiometric amounts of 1,3-diphenylpropane and TEMPO in the absence of solvent were <8%. However, addition of *tert*-butyl alcohol as cosolvent led to better yields of **4**; see Experimental Section. Thermal approaches to the synthesis were unsuccessful, or led to very low yields as a result of biproducts and difficult purification.

Thermal Decomposition. The thermal decomposition of **4** was examined in order to obtain the corresponding kinetics, and from the temperature dependence, the C−O BDE. Further, analysis of the samples served to establish that disproportionation products are not formed.

The study followed along the same lines as our earlier report on the determination of BDEs for **1**−**3**.[8] Briefly, it is necessary to make the bond cleavage of reaction 10 (see Scheme 3) irreversible. This is achieved by adding a second nitroxide in excess, such that recapping yields a different product. In this case we have employed **4**-oxo-TEMPO, as shown in Scheme 3. Plots of conversion as a function of time (see inset in Figure 1) yield the rate constant at a given temperature, and an Arrhenius plot yields the activation energy for reaction

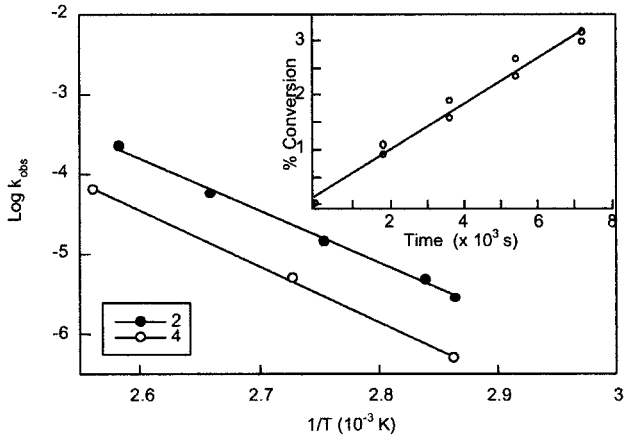

Figure 1. Arrhenius plot of **2** (●) and **4** (○) from thermolysis leading to activation energy and preexponential factor. Inset: Rate constant for **4** obtained at 93.5 °C in the presence of 4-oxo−TEMPO.

Scheme 3

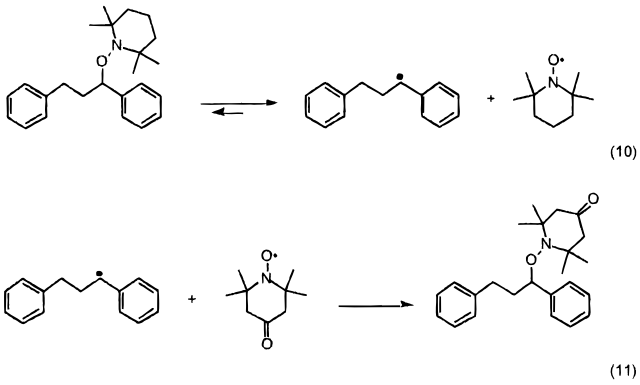

Table 1. Activation Parameters of Various Unimolecular Initiators

initiator	log *A*	E_a(forward) (kJ/mol)	BDE (kJ/mol)
4[a]	13.3	126.7	117.0
2[b]	13.7	128.3	118.7

[a] This work. [b] Literature values.[8]

10. Figure 1 shows the corresponding plot for **4** and also for **2**, which was part of an earlier study.[8] Each point is the average of at least two determinations. The values are compared in Table 1 and are essentially identical to the method of Fukuda derived from oligomers, suggesting our initiators studied are good mimetic compounds for obtaining data from the polymerization process.[21,22] Activation energies are somewhat lower than those reported by Bon et al. for alkoxy-substituted alkoxyamines.[23] The values of the activation energy for **2** and **4** are identical within the experimental error. The small activation energies for the back-reaction are either known or can be estimated on the basis of closely related reactions.[24,25] Combined, they yield the reaction enthalpies that correspond to the bond dissociation energies in the last column of Table 1.

We did not observe any disproportionation products in any of the determinations for **4** used for Figure 1. In contrast, disproportionation products were readily detectable in the case of **2**.

Radical Reactivity of 1,3-Diphenylpropane. The reaction of *tert*-butoxyl radicals with 1,3-diphenylpropane was examined in order to characterize it as a possible source of the benzylic radical from **4**, as well

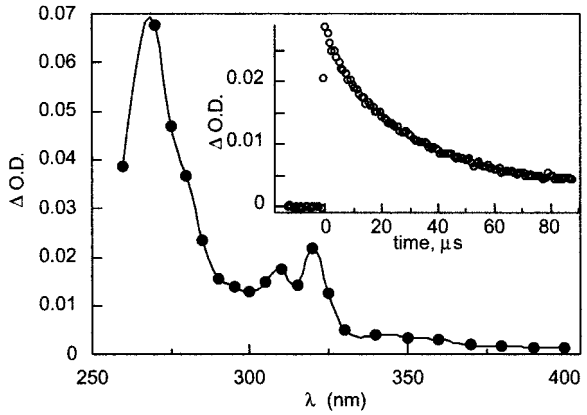

Figure 2. Transient absorption spectrum of substituted 1-phenylethyl radical (**4**•) recorded 10.4 μs after the 266 nm laser pulse. Inset is the decay of the radical in the absence of any quencher recorded at 320 nm.

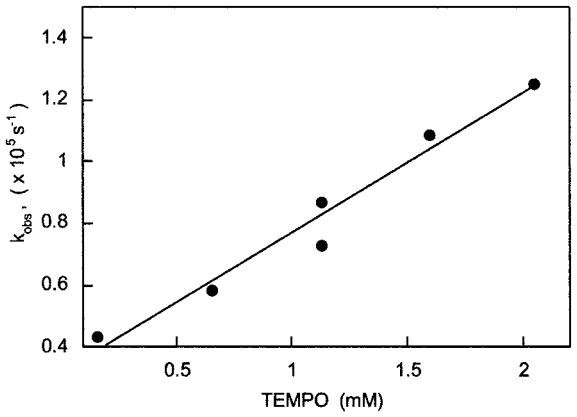

Figure 3. Quenching of 1-phenylethyl radical in the presence of various amounts of TEMPO recorded at 320 nm after 266 nm photolysis.

as to ensure that the reaction (also used for the synthesis of **4**) had the required regioselectivity.

Photolysis of di-*tert*-butyl peroxide (2:1 acetonitrile: peroxide) at 337 nm yielded a transient with $\lambda_{max} = 320$ nm, characteristic of a benzylic radical center. Product studies in the presence of TEMPO showed that abstraction occurred exclusively at the α-position, as expected. The growth signals at 320 nm were too weak to be suitable for an accurate determination of the rate constant for *tert*-butoxyl abstraction from 1,3-diphenylpropane.

The probe method, which has been widely employed to determine *tert*-butoxyl radical rate constants was preferred.[26] The probe was 0.23 M benzhydrol in 4:1 acetonitrile:di-*tert*-butyl peroxide. The deareated solution was excited at 337 nm in the presence of various concentrations of 1,3-diphenylpropane, and the signals form Ph_2C•(OH) monitored at 535 nm. Kinetic analysis led to a rate constant of 1.1×10^6 M^{-1} s^{-1}, virtually identical to that reported for ethylbenzene.[26]

Photoinduced Cleavage of 4. Laser photolysis of **4** in acetonitrile with 266 nm excitation led to the transient spectrum of Figure 2, characteristic of the 1,3-diphenyl-1-propyl radical. In the absence of scavengers its decay was dominated by second-order kinetics (see inset in Figure 2), as expected.

Radical Trapping by TEMPO. The 1,3-diphenyl-1-propyl radical was produced by photolysis of **4** as indicated in the previous section. Addition of TEMPO causes the radical decay to follow pseudo-first-order kinetics, and a plot of the rate constant for decay (k_{obs}) as a function of TEMPO concentration (see Figure 3) yields the corresponding value of k_q from the slope. The value obtained was 4.7×10^7 M^{-1} s^{-1} and is slower than the corresponding value for the 1-phenylethyl radical, which under the same conditions is 1.2×10^8 M^{-1} s^{-1}.[24,25,27]

The value of k_q can also be determined by producing the 1,3-diphenyl-1-propyl radical by H-abstraction by a *tert*-butoxyl radical from 1,3-diphenylpropane. A determination by this method led to a k_q value of 4.0×10^7 M^{-1} s^{-1}. We have established earlier that this method usually yields slightly lower rate constants.[28]

Polymerization Initiated by 2 and 4. Two identical experiments were run at 115 °C in styrene as solvent using **2** and **4** as initiators. The molar ratio of initiator to styrene was 100:1 and the sealed samples were heated for 22 h. The molecular weights (M_n) were 8620 and 8690 for **2** and **4**, respectively, while the polydispersities were 1.16 and 1.12. Clearly, if disproportionation of the growing polymer chain was significant these low polydispersities could not be achieved.

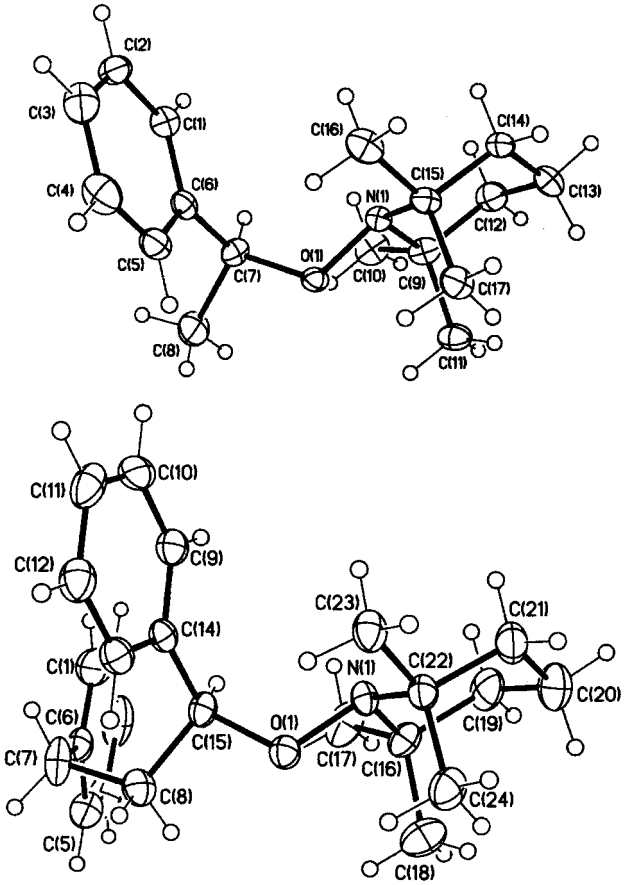

Figure 4. ORTEP diagram of initiators **2** (above) and **4** (below).

Crystallographic Studies. The structures of **2** and **4** were determined by X-ray crystallography. Full details are available as Supporting Information. Figure 4 shows ORTEP diagrams of both molecules.

NMR Studies. Temperature-dependent NMR was used to expand upon other conformational data. The coalescence temperature gives barriers of 68.1 and 69.8 kJ/mol for **2** and **4**, respectively. These values are slightly larger than those reported by Anderson[29] for the benzyl−TEMPO analogue, implying that the barrier

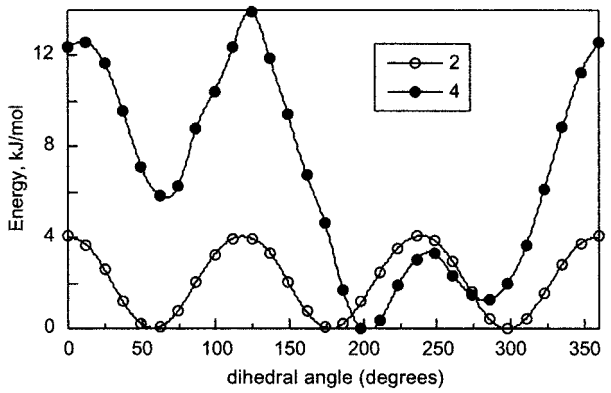

Figure 5. Rotational barrier height for compounds **2** (○) and **4** (●) calculated from semiempirical AM1 coordinate driving with Spartan. The heats of formation (ΔH_f) of each rotamer have been normalized to the lowest energy rotamer.

height increases with substitution on the benzyl center. It is assumed that the rate-determining step for these measurements is the exocyclic bond rotation and does not include any of the other processes such as Walden inversion or ring flipping, which are typically energetically lower.[29,30] We note that these results refer to the O−C bond and not to the key C−C bond (vide infra).

Semiempirical Calculations. Semiempirical calculations were carried out in order to estimate the relative values of the rotational barriers in **2** and **4**. We note that the relevant bond here is the 1−2 C−C bond that controls the stereochemistry for concerted formation of disproportionation products. The structures were minimized with AM1 or PM3 and then the energies for the dihedral angle driver were calculated with the respective level of theory and optimized for every angle. The data are shown in Figure 5. While the absolute values are not reliable, the relative values can be used with a high degree of accuracy to predict trends.[31−33] It is clear that the rotational barrier for **4** is significantly higher, as expected given the substitution pattern in this molecule, having a H_2CCH_2Ph moiety compared with CH_3 from **2**. For AM1 calculations the barrier height is 9.6 kJ/mol higher for **4**, while the difference is 24.2 kJ/mol for PM3.

Discussion

It is clear that the 1,3-diphenyl-1-propyl radical is a typical benzylic radical, as shown by its spectrum, the radical reactivity of the parent 1,3-diphenylpropane, toward *tert*-butoxyl, and the reactivity of the resulting radical toward TEMPO. Further, the C−O BDE in **4** is typical for a secondary benzylic center, and the ability of **4** to initiate polymerization is virtually identical to that of **2**.

Where **2** and **4** differ dramatically is their tendency to form disproportionation products. For **2** at 125 °C, one in 30 cleavage events results in the formation of disproportionation products. Under identical experimental conditions **4** does not lead to any detectable disproportionation products; given current analytical detection limits, disproportionation must be at least 20 times less important for **4** than for **2**. While disproportionation would be difficult to measure in the actual polymer system, any reaction that leads to interruption of polymer growth would lead to a dramatic deterioration of the observed polydispersities. Since this is not the case, it is safe to assume that less than 0.1% of the C−O cleavage events result in disproportionation products.

To discuss the differences in disproportionation products between **2** and **4** it is important to understand the type of mechanism by which the products of reaction 6 are formed. We note that **1** cannot form disproportionation products, while **3** forms them slightly more efficiently than **2**, perhaps a reflection of the increased number of available β-hydrogens.

In principle, there are three mechanisms by which disproportionation products can be formed: (i) by a concerted elimination; (ii) by in-cage reaction within the radical pair formed by C−O cleavage; (iii) by out-of-cage disproportionation between true free radicals. The last of these mechanisms can be ruled out, at least as the main pathway for the formation of disproportionation products. Thermal decomposition of **2** in the presence of other nitroxides (similar to the example of Scheme 3) leads only to characteristic cross-trapped and disproportionation products. The only hydroxylamine formed is that from TEMPO, and not from the nitroxide present in excess,[8,34,35] as would be expected for an out-of-cage disproportionation reaction. The fact that this second nitroxide (typically 4-hydroxy or 4-oxo TEMPO) forms cross-coupling products, but not disproportionation products, implies that out-of-cage cross coupling and disproportionation are not competitive processes.

There is no practical experiment that can distinguish between the other two mechanisms, i.e., concerted or an in-cage radical disproportionation. Even today's ultrafast spectroscopic techniques are unlikely to yield conclusive results. Thus, differentiation between the two mechanisms must be largely based on a critical analysis of the data available.

The rate constant for the reaction of the 1,3-diphenyl-1-propyl radical with TEMPO is 4.7×10^7 M^{-1} s^{-1} in acetonitrile at room temperature. This means that approximately one in 500 radical encounters leads to radical termination, since the rate constant for diffusion-controlled process is acetonitrile is around 2×10^{10} M^{-1} s^{-1}. Even taking into account spin configuration statistics, less than 1% of the singlet encounters lead to a reaction. Thus, the vast majority of the encounters are unreactive and lead to the separation of the two radicals. One can usually assume that in-cage pairs are not dramatically different form those produced by random encounters of free radicals. On this basis, reaction of a geminate radical pair before exit from the original solvent cage must be a remarkably rare event. One would have to argue that geminate pairs are intrinsically different from random pairs; this is an uncommon, but not impossible, argument for a straight recombination reaction, since the radical pair must be born with the perfect orientation for back-reaction.[36,37] But this is not true for disproportionation that requires a radical pair orientation different from the nascent one. Thus, one is forced to the conclusion that this must be a concerted elimination, not involving free or geminate radicals.

The conclusion reached above makes the use of rotational data to interpret the results reasonable. That is, the formation of disproportionation products is the direct result of the decomposition of **2**, and the analogous reaction does not take place for **4**.

Examination of the rotational data for **4** reveals that the barrier that must be overcome, leading to correct

orbital overlap for disproportionation is high compared to **2**. If we assume that concerted elimination requires a syn-periplanar conformation of the H−C−C−O moiety, then it is clear that even if this conformation was not already available, it would be easier to achieve it, the lower the rotational barrier for the C−C bond involved. This can be readily achieved for **2**; in contrast, for **4**, the low energy conformation shows a staggered structure, with the CH_2−Ph group anti-periplanar with respect to the nitroxyl oxygen (see Figure 4). This structure is unfavorable for a four-center elimination, since stereoelectronic factors would not favor the formation of the double bond. Further, the C−O rotational barrier placing the oxygen orbitals in correct alignment for the concerted disproportionation is once again much higher for **4** than for **2**.

Confirmatory evidence for the concerted mechanism comes from the solid-state irradiation of **3**. In solution this initiator is known to undergo significant disproportionation.[8] The diffusion-controlled processes in the solid state are much slower than in solution and could lead to an increase in the amount of observed disproportionation products if an in-cage stepwise mechanism was involved. However, the products obtained after irradiation and thermal decomposition at room temperature are only the free nitroxide and cross-coupled carbon-centered products.[38] The typical hydroxylamine disproportionation products were not detected.

Thus, we believe that the lack of disproportionation of **4** is directly related to its molecular conformation, which is in turn driven by the presence of a large $-CH_2$-Ph substituent. In the actual polymer, this substituent is even larger, thus making disproportionation product formation a virtually impossible reaction, in agreement with the low polydispersities observed.

In summary, while **2** is a good model for the polymer in the context of spectroscopic and kinetic properties, it does not mimic well the formation of disproportionation products. Molecule **4** that incorporates the *penultimate* monomer units has excellent mimetic properties and does not lead to any disproportionation products. The growing capped polymer is also expected to have an anti-periplanar structure between the growing chain and the nitroxyl oxygen, thus preventing elimination leading to disproportionation products.

Experimental Section

Synthesis of 1-(2,2,6,6-Tetramethylpiperidine *N*-oxide)-1,3-diphenylpropane (4). Typical conditions for the photochemical synthesis of **4** consisted of dissolving 500 mg (2.55 mmol) of 1,3-diphenylpropane (Lancaster) and 500 mg (3.20 mmol) of TEMPO (Aldrich), in 5 g (27.2 mmol) of di-*tert*-butyl peroxide (Aldrich) purified through a plug of neutral aluminum oxide (Aldrich). The orange solution was further diluted in 30−35 mL of *tert*-butyl alcohol and placed in a Pyrex test tube, capped, deaereated for a minimum of 20 min with a stream of nitrogen, and irradiated at 300 nm until the orange color no longer persisted, typically 3 days. The lightly colored yellow solution was concentrated under vacuum and the resulting oil was purified by flash chromatography with 5% (v/v) ethyl acetate/hexanes mixture to afford **1** as a solid in 40% yield. ^{1}H NMR (500 MHz, $CDCl_3$, TMS): δ 7.4−7.1 (m, 10H), 4.72−4.40 (m, 1H), 2.51−2.41 (m, 2H), 2.30−2.16 (m, 2H), 1.58 (m, 6H), 1.31 (s, 3H), 1.23 (s, 3H), 1.05 (s, 3H), 0.69 (s, 3H). ^{13}C NMR (300 MHz, $CDCl_3$): δ 143.3, 142.1, 129.6, 128.3, 128.2, 127.97, 127.86, 127.82, 127.04, 125.7, 125.6, 86.9, 59.8, 40.3, 39.5, 37.4, 34.3, 34.2, 33.9, 31.5, 20.2, 17.2. MS (FAB): *m*/*z* (%) 352 (12, M + 1), 268 (2), 193 (5.7), 157 (61.6), 142 (100), 126 (26), 117 (52), 91 (99.8), 69 (44). MS (EI): *m*/*z* (%) 194.1 (18.1), 179 (8.2), 156 (50.7), 142.1 (100), 140 (12.2), 123 (13.3), 117 (37.6), 105 (13.3), 91.1 (96.7), 83.1 (12.4), 69 (42.3), 55 (28.7), 41 (18.8).

Synthesis of 1-(4-Oxo-2,2,6,6-tetramethylpiperidine *N*-oxide)-1,3-diphenylpropane. The same methodology as for **4** was employed, but substituting 4-hydroxy−TEMPO for TEMPO. Under these conditions, the oxidation of the alcohol to the oxo function cannot be controlled. The solid product was isolated and purified with yields similar to those of **4**. ^{1}H NMR (200 MHz, $CDCl_3$, TMS): δ 7.34−7.08 (m, 10H), 4.65 (t, 1H), 3.68−2.34 (m, 4H), 2.32−2.10 (m, 4H), 1.88−1.02 (m, 12H). ^{13}C NMR (300 MHz, $CDCl_3$): δ 210, 142.4, 141.9, 128.5, 128.4, 128.4, 128.2, 127.9, 126.0, 64.93, 63.4, 62.7, 53.9, 53.7, 37.1, 33.9, 33.8, 31.9, 26.6, 22.8, 22.6. MS (FAB): *m*/*z* (%) 366 (57, M + 1), 268 (40), 185 (10), 156 (15), 132 (29), 117 (77), 91 (100), 67 (31).

Synthesis of 1,3-Diphenylpropan-1-ene. To a round-bottom flask was added 148 mg (0.53 mmol) of 1,3-diphenylpropan-1-ol in a 50:50 mixture of methanol/water and was allowed to reflux overnight with 63 mg (15.68 mmol) sodium hydroxide. The sample was separated with dichloromethane, the organic layer dried with anhydrous magnesium sulfate, and concentrated under vacuum. The oil was purified by flash chromatography with 20:1 ethyl acetate/hexanes to afford 30 mg (29%) of the desired compound. ^{1}H NMR (200 MHz, $CDCl_3$, TMS): δ 7.40−7.14 (m, 10H), 6.63 (d, 1H), 6.28 (dd, 1H), 4.08 (m, 2H). MS (EI): *m*/*z* (%) 194 (5), 165 (5), 121 (73), 115 (32), 103(100), 91 (93), 77 (100), 65 (55), 51 (41). This compound was needed as an authentic sample for HPLC analysis.

Synthesis of 1,3-Diphenylpropan-1-one. It was synthesized by pyridinium dichromate (PDC) oxidation of 1,3-diphenylpropan-1-ol by dissolving 73 mg (0.343 mmol) of 1,3-diphenylpropan-1-ol in dichloromethane and 270 mg (0.748 mmol) of PDC (Aldrich). The resulting organic mixture was stirred at room temperature and 1:1 mixture of silica gel, and Celite was added after the reaction was complete. The resulting slurry was filtered and washed with diethyl ether and concentrated under vacuum then purified by flash chromatography with 10% ethyl acetate/hexanes mixture to afford 51 mg of product (71%). Mp: 65−66 °C. ^{1}H NMR (200 MHz, $CDCl_3$, TMS): δ 7.96 (m, 2H), 7.55−7.4 (m, 3H), 7.3−7.19 (m, 5H), 3.34−3.26 (t, 2H), 3.1−3.03 (t, 2H). MS (EI): *m*/*z* (%) 210 (88), 194 (4), 134 (14), 117 (6), 105 (100), 91 (33), 77 (21), 57 (4). ^{13}C NMR (300 MHz, $CDCl_3$): δ 198.2, 140.3, 135.8, 132.1, 127.6, 127.5, 127.4, 127.3, 127.0, 126.9, 125.1, 39.4, 29.1. This compound was needed as an authentic sample for HPLC analysis.

Synthesis of 1,3-Diphenylpropan-1-ol. 3-Phenylpropionaldehyde (530 mg, 3.93 mmol) was dissolved in dry THF (distilled over potassium and benzophenone) and cooled to 0 °C. Phenylmagnesium bromide (1.5 mL, 4.5 mmol) dissolved in dry THF was added dropwise to the 3-phenylpropionaldehyde solution to give another white precipitate that cleared up with time. The reaction was stirred at 0 °C for 5 min, and then ice and water were added to give a white precipitate. The organic layer was washed with a brine solution and then separated with diethyl ether. The organic layer was dried over anhydrous sodium sulfate, concentrated under vacuum, and purified by flash chromatography with 20% ethyl acetate/hexanes to afford 530 mg of the product (64%). ^{1}H NMR (200 MHz, $CDCl_3$, TMS): δ 7.36−7.15 (m, 10H), 4.67 (dd, 2H), 2.72 (m, 2H), 2.11 (t, 2H). ^{13}C NMR (300 MHz, $CDCl_3$): δ 144.5, 141.8, 128.7, 128.6, 128.5, 128.4, 125.9, 73.9, 40.8, 32.1. MS (EI): *m*/*z* (%) 212 (25), 194 (100), 179 (10), 107 (86), 91 (14), 77(13), 65 (3), 51 (3), 32 (2). This compound was needed as an authentic sample for HPLC analysis.

Thermal Decomposition. Determination of the activation energies for thermal decomposition was done as previously reported,[8] where 2 mL of a solution of 18.4 mM of **4** and 51 mM of 4-oxo−TEMPO (to ensure irreversible decomposition) in cyclohexanol were deaereated and flame-sealed in 7 mm test tubes. The samples were then heated in a thermostated aluminum block and were removed at given intervals. The samples were then analyzed for product concentrations by HPLC with a Zorbax C-18 reverse phase column with a flow

rate of 0.5 mL/min and 85% methanol/15% water as eluent. The retention times and peak areas were calibrated against the authentic samples. The rate constants were derived from product formation as a function of time over a series of temperatures. The subsequently generated Arrhenius plot represents the average of two determinations at each temperature.

Laser Flash Photolysis Studies. Several laser techniques were employed in studies of the radical reactivity of intermediates derived from **4**. Briefly, our system employs several pulsed lasers as excitation sources (vide infra). The signals from the monochromator/photomultiplier system were initially captured by a Tektronix 2440 digitizer and transferred to a Power Macintosh computer that controlled the experiment with software developed in the LabVIEW 4.1 environment from National Instruments. Other aspects of the system are similar to those described earlier.[39,40]

The radical reactivity of 1,3-diphenylpropane was examined by generating *tert*-butoxyl radicals from the peroxide using the 337 nm pulses (~10 ns, <5 mJ/pulse) from a Molectron UV-24 nitrogen laser or with the third harmonic (355 nm, ~6 ns, <35 mJ/pulse) from a Continuum Surelite Nd:YAG laser. The photoinduced cleavage of **4** was examined using the 266 nm pulses from the fourth harmonic (~6 ns, <20 mJ/pulse) from a similar Surelite laser. The same laser source was employed for radical trapping studies using TEMPO.

Initiation of Polymerization by 2 and 4. Polymerization reactions were carried out using freshly distilled styrene as solvent/reactant. The initiators, **2** or **4**, were dissolved in 100 equiv of styrene and flame-sealed under vacuum in a 7 mm glass tube after two cycles of freeze−pump−thaw. They were then heated in a thermostated aluminum block at 115 °C for 22 h. The samples were cooled, and any residual styrene was evaporated under vacuum; the resulting oil was then dissolved in THF and then analyzed by gel permeation chromatography in a Varian HPLC instrument equipped with a Waters Styragel HR3 column and RI detector. The molecular weights and polydispersities were determined relative to polystyrene molecular weight standards.

X-ray Crystallography. Structural Determination of 1 and 2. Crystallographic details are reported in the Supporting Information. Suitable crystals were selected, mounted on thin, glass fibers using paraffin oil and cooled to the data collection temperature. Data were collected on a Brüker AX SMART 1K CCD diffractometer using 0.3° ω scans at 0, 90, and 180° in ϕ. Unit-cell parameters were determined from 60 data frames collected at different sections of the Ewald sphere. No absorption corrections were required.

Systematic absences in the diffraction data and unit-cell parameters were uniquely consistent with the reported space group. The structure was solved by direct methods, completed with difference Fourier syntheses, and refined with full-matrix least-squares procedures based on F^2. All non-hydrogen atoms were refined with anisotropic displacement parameters. Phenyl groups were treated as idealized, rigid, flat hexagons. Hydrogen atoms on carbon atom C(8) in **1** were initially located from the difference map and refined with a riding model. All other hydrogen atoms were treated as idealized contributions. All scattering factors and anomalous dispersion factors are contained in the SHEXTL 5.10 program library (Sheldrick, G. M.; Bruker AXS, Madison, WI, 1997).

NMR Studies. ^{1}H DNMR of **1** and **2** was done in C_6D_6 and $CDCl_3$ on a 500 MHz Brüker NMR in the temperature range of 298−348 K. The rotational barrier was determined from coalescent temperatures according to reported methods.[29,30]

Semiempirical Calculations. Semiempirical calculations were carried out on a Silicon Graphics Indigo workstation using Spartan SGI version 4.0.4 GL IRX 5.2. The rotational barriers were calculated using the coordinate driving option with the PM3[32] and AM1[41] semiempirical levels of theory that calculated the optimized geometries and heats of formation (ΔH_f) for the particular dihedral angle. Restricted Hartree−Fock (RHF) was selected for the calculations for all systems, and the σ value was set at 100.

Acknowledgment. J.C.S. thanks the Natural Sciences and Engineering Research Council of Canada for support, and the Instituto de Tecnología Química (Valencia) where this article was completed while J.C.S. was a guest under the auspices (grant SAB1998-0121) of the Ministerio de Educación y Ciencia (Spain). W.G.S. would like to acknowledge NSERC for support through a graduate scholarship. We thank Dr. Roger Sinta for putting us on the penultimate track and R. Capoor for his assistance with the DNMR measurements.

Supporting Information Available: Tables of crystal structures for **2** and **4**, including figures showing structures, and a table of kinetic data for Figure 1. This material is available free of charge via the Internet at http://pubs.acs.org.

References and Notes

(1) Hawker, C. J. *Acc. Chem. Res.* **1997**, *30*, 373.
(2) Matyjaszewski, K. In *Controlled Radical Polymerization*; Matyjaszewski, K., Ed.; American Chemical Society: Washington, DC, 1998; Vol. 685; p 2.
(3) Roberts, J. R.; Ingold, K. U. *J. Am. Chem. Soc.* **1973**, *95*, 3228.
(4) Solomon, D. H.; Rizzardo, E.; Cacioli, P. US Patent 4,581,429, 1986.
(5) Moad, G.; Rizzardo, E.; Solomon, D. H. *Polym. Bull.* **1982**, *6*, 589.
(6) Georges, M. K.; Veregin, R. P. N.; Kazmaier, P. M.; Hamer, G. K. *Macromolecules* **1993**, *26*, 2987.
(7) Veregin, R. P. N.; Georges, M. K.; Kazmaier, P. M.; Hamer, G. K. *Macromolecules* **1993**, *26*, 5316.
(8) Skene, W. G.; Belt, S. T.; Connolly, T. J.; Hahn, P.; Scaiano, J. C. *Macromolecules* **1998**, *31*, 9103.
(9) Ciriano, M. V.; Korth, H.-G.; van Scheppingen, W. B.; Mulder, P. *J. Am. Chem. Soc.* **1999**, *121*, 6375.
(10) Le Mercier, C.; A.; G.; Tordo, P.; Marque, S.; Martschke, R.; Fischer, H. *Polym. Prepr.* **1999**, *40*, 313.
(11) Veregin, R. P. N.; Odell, P. G.; Michalak, L. M.; Georges, M. K. *Macromolecules* **1996**, *29*, 2746.
(12) Georges, M. K.; Veregin, R. P. N.; Daimon, K. In *Controlled Radical Polymerization*; Matyjaszewski, K., Ed.; American Chemical Society: Washington, DC, 1998; Vol. 685, p 170.
(13) Hawker, C. J.; Barclay, G. G.; Orellano, A.; Dao, J.; Devonport, W. *Macromolecules* **1996**, *29*, 5245.
(14) Howard, J. A.; Tait, J. C. *J. Am. Chem. Soc.* **1978**, *43*, 4279.
(15) Li, I.; Howell, L. *Macromolecules* **1995**, *28*, 6692.
(16) Fischer, H. *J. Am. Chem. Soc.* **1986**, *108*, 3925.
(17) Kothe, T.; Marque, S.; Martschke, R.; Popov, M.; Fischer, H. *J. Chem. Soc., Perkin Trans. 2* **1998**, *7*, 1553.
(18) Fischer, H. *J. Polym. Sci., Part A: Polym. Chem.* **1999**, *37*, 1885.
(19) The ideal model would have one more methyl group, but this would require a significant increase in the synthetic effort.
(20) Connolly, T. J.; Baldovi, M. V.; Mohtat, N.; Scaiano, J. C. *Tetrahedron Lett.* **1996**, *37*, 4919.
(21) Fukuda, T.; Goto, A. *Macromol. Rapid Commun.* **1997**, *18*, 683.
(22) Goto, A.; Rerauchi, T.; Fukuda, T.; Miyamoto, T. *Macromol. Rapid Commun.* **1997**, *18*, 373.
(23) Bon, S. A. F.; Chambard, G.; German, A. L. *Macromolecules* **1999**, *32*, 2, 8269.
(24) Beckwith, A. J.; Bowry, V. W.; Ingold, K. U. *J. Am. Chem. Soc.* **1992**, *114*, 4983.
(25) Bowry, V. W.; Ingold, K. U. *J. Am. Chem. Soc.* **1992**, *114*, 4992.
(26) Paul, H.; Small, R. D., Jr.; Scaiano, J. C. *J. Am. Chem. Soc.* **1978**, *100*, 4520.
(27) Chateauneuf, J.; Lusztyk, J.; Ingold, K. U. *J. Org. Chem.* **1988**, *53*, 1629.
(28) Skene, W. G.; Scaiano, J. C.; Listigovers, N. A.; Kazmaier, P. E.; Georges, M. K. *Macromolecules* **1999**, submitted for publication.
(29) Anderson, J. E.; Casarinin, D.; Corrie, J. E. T.; Lunazzi, L. *J. Chem. Soc., Perkin Trans. 2* **1993**, *7*, 1299.
(30) Anderson, J. E.; Corrie, J. E. T. *J. Chem. Soc., Perkin Trans. 2* **1992**, *7*, 1027.

(31) Fabian, W. M. F. *J. Comput. Chem.* **1988**, *9*, 369.
(32) Stewart, J. J. P. *J. Comput. Chem.* **1989**, *10*, 209.
(33) Stewart, J. J. P. *J. Comput. Chem.* **1989**, *10*, 221.
(34) Skene, W. G.; Scaiano, J. C. *J. Phys. Chem.* **2000**, submitted for publication.
(35) Moffat, K. A.; Hamer, G. K.; Georges, M. K. *Macromolecules* **1999**, *32*, 1004.
(36) Benson, S. W. In *Advances in Photochemistry*; Noyes, W. A. J., Hammond, G. S., Pitts, J. N. J., Eds.; John Wiley & Sons: New York, 1964; Vol. 2, p 1.
(37) Tanner, D. D.; Rahimi, P. M. *J. Am. Chem. Soc.* **1982**, *104*, 225.
(38) Skene, W. G.; Scaiano, J. C. Unpublished results.
(39) Scaiano, J. C. *J. Am. Chem. Soc.* **1980**, *102*, 7747.
(40) Scaiano, J. C.; Tanner, M.; Weir, D. *J. Am. Chem. Soc.* **1985**, *107*, 4396.
(41) Dewar, M. J. S.; Zoebisch, E. G.; Healy, E. F.; Stewart, J. J. P. *J. Am. Chem. Soc.* **1985**, *107*, 3902.

MA991924D